

Regular paper

**Determination of the Performance
Extreme Values of a Three-phase
Induction Machine Using Algebraic
and Graphical Methods**

This paper proposes an algebraic and a graphical method for finding all the performance extreme values of a three-phase induction machine when it operates as a motor or a generator. The performance extreme include maximum efficiency, maximum power factor, maximum electric power, maximum torque and maximum mechanical power in both motoring and generating modes. In addition to the algebraic method, this paper shows how an old graphical method can be used to accurately find the performance extreme values of a three-phase induction machine. With the use of modern graph drawing software that draws geometric graphs with their parameters as accurate as four places past the decimal, the circle diagram method, which is not well known to most young electrical engineers, merits a new reevaluation of its usefulness. Comparison between algebraic and graphical calculations shows that in most cases the relative errors of the proposed graphical method are less than one percent.

Keywords: induction machine, circle diagram method, performance extreme values.

1. Introduction

Analysis of the steady-state performance of a three-phase induction machine can be achieved by analyzing its equivalent circuit. In most cases, as long as the parameters of the equivalent circuit are known, the operating characteristics of the machine such as power factor, efficiency, input power, output power, and torque, at a given slip, can be calculated.

Among these performance characteristics, the maximum torque is the most often discussed extremum in textbooks of electric machines (e.g., [1]-[2]). On the other hand, other performance extrema are rarely documented. Although the maximum torque is the most important performance extremum to be considered, other performance extrema may also be of importance in some applications. For example, when energy saving is the objective to be achieved, the slip at which the maximum efficiency occurs is of interest. The performance extreme values of an induction machine also provide a valuable guide both to machine designers and to power engineers. Machine designers can see the effects of modifying one or several machine design parameters on the performance limits of the machine. Similarly, power engineers can quickly know whether a machine can safely be operated under a specific condition.

The information on maximum efficiency and maximum power factor is helpful for the induction motor designer to make a compromise between high power factor and high efficiency. Typically, the rated slip of an induction motor falls somewhere between maximum efficiency and maximum power factor. Maximum torque and maximum output power are two important mechanical characteristics of a motor. If a motor's load torque is

Corresponding author : S.Y. Huang
Unité de recherche en CSSS, Graduate School of Engineering Science and Technology (Doctoral Program),
National Yunlin University of Science & Technology, 123 University Road, Section 3, Douliou, Yunlin 64002,
Taiwan, R.O.C.
E-mail: g8910814@yuntech.edu.tw

increased beyond the maximum torque, the motor will stall and come to a rapid stop. Hence, high maximum (pullout) torque is necessary for applications that may undergo frequent overloading. Maximum output power is a performance indicator when the motor is used as a mechanical power source in an electric (or hybrid) vehicle. Maximum output power of the motor is often compared with that of a conventional engine. When an induction machine operates as a generator, its maximum torque (also known as pushover torque) and maximum input power are two critical mechanical limits beyond which the torque and power applied by the prime mover can cause overspeed to the generator and may damage it.

In this paper, the performance extreme values of a three-phase induction machine working in both motoring and generating modes (*c.f.*, **Fig. 1**) are derived first by algebraically solving the equivalent circuit shown in **Fig. 2**. These extreme values include maximum torque, maximum mechanical power, maximum power factor, maximum efficiency, and maximum electric power. It will be shown that the torque and mechanical power extrema can be expressed in analytical forms while the power factor, efficiency and electric power extrema need to be solved numerically. It will then be shown that these extrema can also be determined graphically using the circle diagram method. The circle diagram method is an old method but can still be found in some textbooks (*e.g.*, [3]-[4]). The research into graphical methods for induction motor analysis is still active (*e.g.*, [5]-[11]). One may consider that the circle diagram method is limited to qualitative evaluation because it cannot give accurate results. In fact, if the circle diagram method is carried out by a modern computer drawing tool that allows the user to draw geometric diagrams with parameters (*i.e.*, coordinates, lengths, angles, etc.) to the accuracy of four decimal places, then the circle diagram method is able to give all the aforementioned performance extrema with required accuracy. Unlike the circle diagram method used in [10] and [11] that is based on the approximate equivalent circuit of induction machine and is limited to motoring mode of operation, the circle diagram method used in this paper is based on the accurate equivalent circuit and covers both motoring and generating modes. An example will be illustrated and the results obtained from the algebraic and graphical methods will be compared.

2. Operating modes and equivalent circuit of an induction machine

Fig. 1 shows the typical torque-speed characteristic of an induction machine. The machine operates as a motor for a slip s ranging from zero to one, as a generator for a negative s , and as a brake for s greater than one. The single-phase equivalent circuit of a three-phase induction motor is shown in Fig. 2 where r_1 and x_1 are the stator resistance and reactance, r_2 and x_2 the stator-referred rotor resistance and reactance, r_{fe} and x_M the core-loss resistance and magnetizing reactance, V_1 is the phase voltage of the stator, V_2' is the air-gap voltage. The circuit of Fig. 2 is sometimes called the T-type equivalent circuit, which is to be distinguished with the L-type equivalent circuit that is an approximate equivalent circuit achieved by moving the magnetizing branch to the machine terminals.

In the following analysis, the T-type equivalent circuit will be used. It should be noted that the motor convention is used in Fig. 2 when the machine operates as an induction motor (IM). However, when the machine operates as an induction generator (IG), the generator convention is used and the directions of currents I_1 and I_2 in Fig. 2 have to be reversed

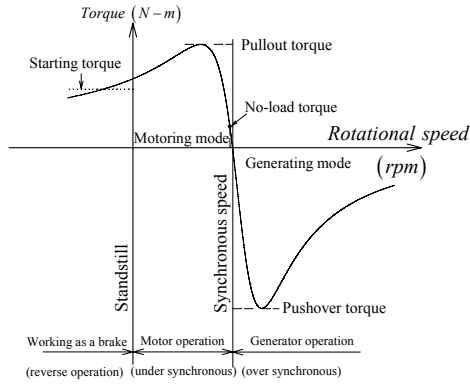


Fig. 1: Typical torque-speed characteristic of an induction machine

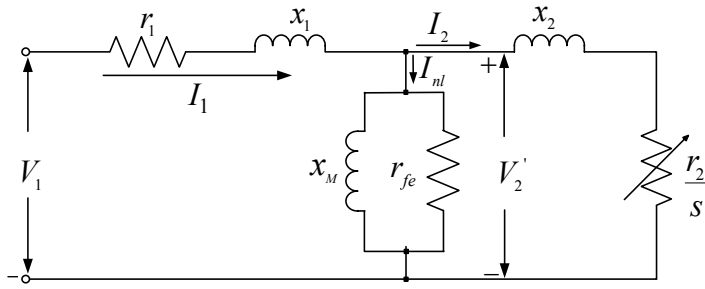


Fig. 2 : Per-phase equivalent circuit of a three-phase induction motor

3. Algebraic analysis

The equivalent circuit of Fig. 2 is analyzed algebraically for finding the characteristic extreme values when the machine operates as a motor or a generator. To facilitate analysis, the stator side and the magnetizing portion are replaced by a voltage source V_{th} in series with an impedance $Z_{th} = r_{th} + jx_{th}$ using the Thevenin's theorem, as shown in **Fig. 3**.

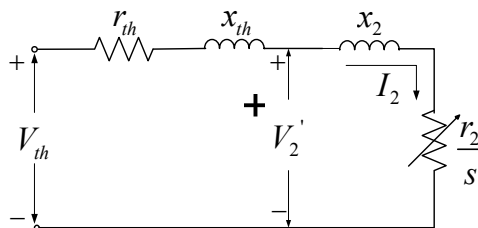


Fig. 3: Induction-motor equivalent circuit simplified by Thevenin's theorem

A 3.1. Maximum torque

The developed torque is a maximum when the power delivered to r_2/s in Fig. 3 is maximum [2]. The maximum power transfer theorem implies that the air-gap power will be greatest when the resistance r_2/s equals the magnitude of the impedance $r_{th}+j(x_{th}+x_2)$. Let the slip at maximum torque be s_T , then the following condition holds

$$\left| r_{th} + j(x_{th} + x_2) \right| = r_2/s_T. \quad (1)$$

The slip at maximum torque is then given by

$$s_T = \frac{\pm r_2}{\sqrt{\left(r_{th}^2 + (x_{th} + x_2)^2 \right)}} \quad (2)$$

where the plus (minus) sign applies to the motoring (generating) mode. The torque τ is the power delivered to the resistance $r_2(1-s)/s$ divided by the rotor mechanical angular velocity ω_m , which is equivalent to the power consumed by the resistance r_2/s divided by the synchronous mechanical angular velocity ω_s

$$\tau = 3I_2^2 \left(\frac{1-s}{s} \right) r_2 / \omega_m = \frac{3I_2^2 (r_2/s)}{\omega_m/(1-s)} = \frac{3I_2^2 (r_2/s)}{\omega_s} \quad (3)$$

With the slip s_T known, the corresponding torque can be found by inserting (2) into (3)

$$\tau = \frac{3}{2\omega_s} \cdot \frac{V_{th}^2}{\sqrt{r_{th}^2 + (x_{th} + x_2)^2} \pm r_{th}} \quad (4)$$

where the plus (minus) sign applies to the motoring (generating) mode. We use s_{TM} (s_{TG}) to refer to the slip at maximum torque in motoring (generating) mode. We use τ_M (τ_G) to refer to the corresponding maximum torque in motoring (generating) mode, which is also known as pullout (pushover) torque.

B 3.2. Maximum mechanical power

The mechanical power of an induction machine refers to its output (input) power as it operates as an IM (IG). The maximum mechanical power can be obtained in a similar way to the maximum torque. In Fig. 2, the resistance r_2/s can be separated into r_2 and $r_2(1-s)/s$ to take into account the rotor copper loss and the electromechanical power respectively. The resistance $r_2(1-s)/s$ dissipates a maximum power when it is equal to the magnitude of the impedance $(r_{th}+r_2)+j(x_{th}+x_2)$. Thus, the slip at maximum mechanical power is given by

$$s_{mp} = \frac{r_2 \cdot \left(-r_2 \pm \sqrt{(r_2 + r_{th})^2 + (x_2 + x_{th})^2} \right)}{r_{th} (2r_2 + r_{th}) + (x_2 + x_{th})^2} \quad (5)$$

where the plus (minus) sign applies to the maximum output (input) mechanical power of the IM (IG). We use s_{mp_M} (s_{mp_G}) to refer to the slip at the maximum output (input) power of an IM (IG). The output (input) mechanical power of a three-phase IM (IG) can be written as

$$P_m(s) = 3I_2^2 \left| \frac{1-s}{s} \right| r_2 \quad (6)$$

Substituting s_{mp_M} (s_{mp_G}) into (6) yields the maximum output (input) power of the motor (generator). We use P_{mM} (P_{mG}) to refer to the maximum output (input) mechanical power of the IM (IG). The absolute value sign in (6) serves to give a positive value of power when the machine is in generating mode ($s < 0$).

C 3.3. Maximum power factor

The impedance looking into the stator terminals in Fig. 2 can be written as a function of the slip s

$$Z(s) = (r_1 + jx_1) + \left[\left(\frac{1}{r_{fe}} + \frac{1}{jx_M} \right) + \left(\frac{r_2}{s} + jx_2 \right) \right]^{-1} \quad (7)$$

The tangent of the angle θ_1 of the impedance $Z(s)$ is given by

$$\tan \theta_1 = \text{Im}(Z(s)) / \text{Re}(Z(s)) \quad (8)$$

When the machine operates as a motor or a brake ($s > 0$), the impedance angle θ_1 must be included in the interval $[0, \pi/2]$; when the machine operates as a generator ($s < 0$), θ_1 is in the interval $[\pi, 3\pi/2]$. Over the two intervals, $\tan \theta_1$ is a strictly increasing function of θ_1 , and $\cos \theta_1$ is a strictly decreasing function of θ_1 , although $\tan \theta_1$ has a discontinuity at $\theta_1 = \pi/2$. It follows that the local minimum of θ_1 must occur at the local minimum of $\tan \theta_1$, and also at the local maximum of $\cos \theta_1$. In other words, finding the minimum of $\tan \theta_1$ is equivalent to finding the maximum of the power factor $\cos \theta_1$. Accordingly, the slip at maximum power factor can be obtained by equating the derivative of $\tan \theta_1$ to zero

$$\frac{d}{ds}(\tan \theta_1) = \frac{d}{ds} \frac{\text{Im}(Z(s))}{\text{Re}(Z(s))} = 0 \quad (9)$$

Solving (9) for s gives two distinct real roots. The positive (negative) root s_{PF_M} (s_{PF_G}) is the slip at maximum power factor in the motoring (generating) mode. The respective values of the corresponding maximum power factors, denoted by PF_M and PF_G , can be determined by inserting s_{PF_M} and s_{PF_G} into the following equation

$$PF = \cos \left(\tan^{-1} \left(\frac{\text{Im}(Z(s))}{\text{Re}(Z(s))} \right) \right) \quad (10)$$

It is noted that numerical calculation is needed for the resolution of (9).

D 3.4. Maximum efficiency

The electric power of an induction machine refers to its input (output) power as it operates as an IM (IG). Referring to the equivalent circuit of Fig. 2, the electric power of the machine can be expressed as

$$P_e(s) = 3 \left| I_1^2 r_1 + I_2^2 \frac{r_2}{s} + \frac{(V_2')^2}{r_{fe}} \right| \quad (11)$$

where the absolute value sign ensures a positive value for generating mode ($s < 0$), and referring to Fig. 3, the air-gap voltage V_2' can be given by

$$V_2' = V_{th} \frac{r_2/s + jx_2}{(r_{th} + r_2/s) + j(x_{th} + x_2)} \quad (12)$$

The efficiency of the machine η is calculated differently according to its mode of operation

$$\eta(s) = \begin{cases} \eta_m = P_m/P_e, & s \geq 0 \\ \eta_g = P_e/P_m, & s < 0 \end{cases} \quad (13)$$

where P_m and P_e are given by (6) and (11). The slip at maximum efficiency of the machine can be determined by equating the derivative of η to zero

$$\frac{d}{ds} \eta(s) = 0 \quad (14)$$

Solving (14) for s , we obtain two roots. The positive (negative) root s_{η_M} (s_{η_G}) is the slip at maximum efficiency in motoring (generating) mode. Inserting s_{η_M} (s_{η_G}) into (13) allows the maximum efficiency η_M (η_G) of the motor (generator) to be calculated. It is noted that (14) is solved numerically in this paper.

E 3.5. Maximum electric power

The electric power of the induction machine has been given by (11). The maximum electric power of the machine can be found by equating the derivative of P_e with respect to s to zero.

$$\frac{d}{ds} P_e(s) = 0 \quad (15)$$

Two roots to (15) will be found. The positive (negative) root s_{ep_M} (s_{ep_G}) is the slip at the maximum input (output) power of an IM (IG). We use P_{eM} (P_{eG}) to refer to the corresponding maximum input (output) electric power of an IM (IG), which can be determined by inserting s_{ep_M} (s_{ep_G}) into (11).

4. Graphical analysis

In the previous algebraic analysis, while analytical solutions to the extrema of torque and mechanical power can be found, we need to resort to numerical methods to find the extrema of power factor, efficiency and electric power. On the other hand, the proposed graphical method finds these extrema by identifying the longest line segments or the smallest angle in the circle diagram, which is easier and far more intuitive.

F 4.1. Construction of an exact circle diagram

The basic principle of the circle diagram is that the current locus of a series $R-L$ circuit is a circle when L is fixed and R is variable. **Fig. 4** shows a series $R-L$ circuit supplied by a voltage V_p . The current I_p is given by

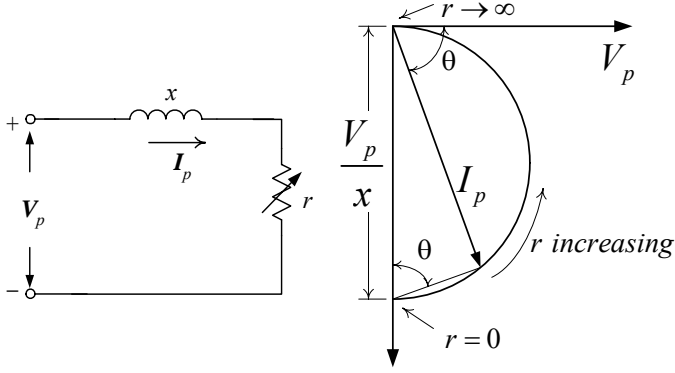


Fig. 4 : A series $R-L$ circuit and the locus of the current

$$I_p = \frac{V_p}{|r + jx|} = \frac{V_p}{x} \frac{x}{\sqrt{r^2 + x^2}} = \frac{V_p}{x} \sin \theta \quad (16)$$

where θ is the angle of the impedance $r+jx$. The locus of I_p in the complex plane is a semicircle of diameter V_p/x . This principle can readily be applied to construct the circle diagram of the circuit shown in Fig. 2. The construction of an exact circle diagram requires that an angle μ and the stator current (magnitude and phase angle) at no-load and at blocked-rotor tests be known. The angle μ is the angular phase difference between the phase terminal voltage V_1 and air-gap voltage V_2' under no-load condition. Referring to **Fig. 5**, the procedure proceeds as follows.

- 1) Draw $\overline{OV_1}$ on the horizontal axis to represent the phase voltage V_1 . Draw the no-load test current $I_{nl}(\overline{ON})$ and the blocked-rotor test current $I_{IBR}(\overline{OB})$.
- 2) Draw a dashed line $N'D'$ passing through N and parallel to the vertical axis. From N draw a line ND which must be set off at an angle 2μ from $\overline{ND'}$ [9].
- 3) Join \overline{NB} to obtain the rotor current at blocked-rotor test I_{2BR} . The perpendicular bisector of NB intersects ND at C . Draw a circle with center C and radius \overline{NC} .
- 4) Draw a line vertical to ND passing through B and intersecting the vertical axis and ND at G and U .
- 5) Divide \overline{UB} at W in the ratio of $\overline{UW} : \overline{WB} = r_1' : r_2$, where r_1' is r_1 reduced in the ratio of no-load V_2' to V_1 [4].

$$r_1' = r_1 \left| \frac{V_2' (no-load)}{V_1} \right| \quad (17)$$

- 6) Join \overline{NW} and extend \overline{NW} to intersect the circle at T . Line NT is called the torque line and line NB the output line.

Points N , B and T on the circle refer to slips of zero, one and infinity, respectively. For an IM working at a slip $0 \leq s \leq 1$ with operating point K as shown in **Fig. 5**, from K we draw a line perpendicular to ND and intersecting other line segments at points A , E , Q and J . The following performance characteristics of the IM can be expressed by the lengths and angles of line segments of the circle diagram:

$$P_e = 3V_1 \overline{AK} \quad (18)$$

$$P_m = 3V_1 \overline{JK} \quad (19)$$

$$\tau = P_m / [(1-s) \omega_s] = 3V_1 \overline{QK} / \omega_s \quad (20)$$

$$s = \overline{QJ} / \overline{QK} \quad (21)$$

$$\eta_m = P_m / P_e = \overline{JK} / \overline{AK} \quad (22)$$

$$PF = \cos \theta_1 \quad (23)$$

Similarly, for an IG operating at point K' , from K' we draw a line perpendicular to ND and intersecting other line segments at points A' , E' , Q' and J' . The performance characteristics of the IG can be expressed as follows.

$$P_m = 3V_1 \overline{J'K'} \quad (24)$$

$$P_e = 3V_1 \overline{A'K'} \quad (25)$$

$$\tau = P_m / [(1-s) \omega_s] = 3V_1 \overline{Q'K'} / \omega_s \quad (26)$$

$$s = -\overline{Q'J'} / \overline{Q'K'} \quad (27)$$

$$\eta_g = P_e / P_m = \overline{A'K'} / \overline{J'K'} \quad (28)$$

$$PF = |\cos \theta_1'| \quad (29)$$

are the tangent points of two lines parallel to the torque line and the circle. Points P_4 and P_4' in Fig. 6(a) refer to the operating points of maximum torque for the IM and IG respectively. The slips s_{TM} and s_{TG} at P_4 and P_4' can be given respectively by

$$s_{TM} = \overline{a_3 a_4} / \overline{a_3 P_4} \quad (34)$$

$$s_{TG} = -\overline{b_1 b_2} / \overline{b_1 P_4'} \quad (35)$$

The pullout torque τ_M and the pushover torque τ_G are given by

$$\tau_M = 3V_1 \overline{a_3 P_4} / \omega_s \quad (36)$$

$$\tau_G = 3V_1 \overline{b_1 P_4'} / \omega_s \quad (37)$$

I 4.4. Maximum mechanical power

In Fig. 5, the segment to the right (left) of the output line, \overline{JK} ($\overline{J'K'}$), determines the output (input) mechanical power of the machine (cf. (19) and (24)) as it operates as a motor (generator). Hence, point P_3 (P_3') in Fig. 6(a) at which a line parallel to \overline{NB} is tangent to the circle in the motoring (generating) region, refers to the operating point of maximum output (input) mechanical power. The slips s_{mM} and s_{mG} at P_3 and P_3' are given by

$$s_{mp_M} = \overline{a_1 a_2} / \overline{a_1 P_3} \quad (38)$$

$$s_{mp_G} = -\overline{b_3 b_4} / \overline{b_3 P_3'} \quad (39)$$

The corresponding maximum mechanical power P_{mM} and P_{mG} are

$$P_{mM} = 3V_1 \overline{a_2 P_3} \quad (40)$$

$$P_{mG} = 3V_1 \overline{b_4 P_3'} \quad (41)$$

J 4.5. Maximum Power Factor

When the machine works as a motor, segment \overline{OK} in Fig. 5 refers to the stator current I_1 . The angle θ_1 between \overline{OK} and $\overline{OV_1}$ is the power factor angle. A smallest power factor angle implies a maximum power factor. The smallest power factor angle occurs when \overline{OK} is tangent to the circle in the motoring region. In Fig. 6(a), a line passing through O is tangent to the circle at P_2 , which is the operating point of the motor with maximum power factor since θ_{1M} is smallest. **Fig. 6(b)** is an enlarged view of the area around the point N of Fig. 6(a). With reference to Fig. 6(b), the slip at maximum power factor of the motor is

$$s_{PF_M} = \overline{c_4 c_5} / \overline{c_4 P_2} \quad (42)$$

The maximum power factor of the motor (PF_M) is simply $\cos \theta_{1M}$ where the angle θ_{1M} is

formed by $\overline{OV_1}$ and $\overline{OP_2}$ as shown in Figs. 6(a) and (b).

Similarly, when the machine works as a generator, the angle θ_1' between $\overline{OK'}$ and $\overline{OV_1}$ is the power factor angle. When $\overline{OK'}$ is tangent to the circle, the machine works at maximum power factor. The tangent point P_2' in Fig. 6(a) shows the working point of maximum power factor. With reference to Fig. 6(b), the slip at maximum power factor of the generator is

$$s_{PF_G} = -\overline{c_8c_9} / \overline{c_8P_2'} \quad (43)$$

The maximum power factor of the generator (PF_G) is the absolute value of $\cos\theta_{1G}$ where the angle θ_{1G} is formed by $\overline{OV_1}$ and $\overline{OP_2'}$ as shown in Fig. 6(b).

K 4.6. Maximum Efficiency

To find the operating point of maximum efficiency in Fig. 6(b), we extend the output line NJ toward upper left to intersect the vertical axis at M . From M , we draw two lines tangent to the circle in motoring region at P_1 and in generating region at P_1' . Points P_1 and P_1' are the working points of maximum efficiency of the machine when it works as a motor or a generator, respectively. This result is less evident than the other operating points of extrema. The proof of the construction of the graph for finding the maximum efficiency point of an IM has been given in [11]. The proof for an IG can be carried out in a similar way. The slips s_{η_M} and s_{η_G} at maximum efficiency can be given by

$$s_{\eta_M} = \overline{c_2c_3} / \overline{c_2P_1} \quad (44)$$

$$s_{\eta_G} = -\overline{c_6c_7} / \overline{c_6P_1'} \quad (45)$$

The corresponding maximum efficiencies η_M and η_G can be written as

$$\eta_M = \overline{c_3P_1} / \overline{c_1P_1} \quad (46)$$

$$\eta_G = \overline{c_{10}P_1'} / \overline{c_7P_1'} \quad (47)$$

L 5.1. Graphical calculation

The construction procedure of an exact circle diagram outlined in section 4.1 can be followed to draw the circle diagram of the induction machine as shown in Fig. 7(a). Modern graph drawing software allows the user to draw lines, arcs, curves, circles, etc. and can show their geometric parameters (*i.e.*, coordinates, position, length, angle, size, etc.) as accurate as four (or more) places past the decimal point [12]. This feature largely enhances the accuracy of a graphical method. The idea that the circle diagram method can only be used for qualitative analysis of an induction machine, is no more valid in view of improvement in performance of state-of-the-art graph drawing tools.

In **Fig. 7(a)**, the source phase voltage $V_1 = 220 / \sqrt{3} V$ is drawn on the horizontal axis on a scale of $4 V/mm$, so the length of $\overline{OV_1}$ is $31.7543 mm$. From the parameters of the equivalent circuit, the stator current at no-load and at blocked-rotor tests can be given by

$$I_{nl} = 4.293 \angle -83.9325^\circ A$$

$$I_{LBR} = V_1 / [(r_1 + jx_1) + ((r_{fe}) / (jx_M)) / (r_2 + jx_2)] = 40.8535 \angle -54.9994^\circ A$$

The angle μ is given by

$$V_2' = V_1 ((r_{fe}) / (jx_M)) / [((r_{fe}) / (jx_M)) + (r_1 + jx_1)] = 121.29 \angle 1.5477^\circ V \quad , \quad \text{under no-load condition.}$$

$$\mu = 1.5477^\circ$$

And the adjusted stator resistance, r_1' , is

$$r_1' = r_1 |V_2'| / |V_1| = 0.83364 \Omega$$

The current phasors are drawn on a scale of $0.5 A/mm$. Both the voltage and current scales are shown at the lower right corner in Fig. 7(a).

The procedure for determining the performance extrema outlined in sections 4.2-4.6 can be followed to find ten corresponding operating points P_1-P_5 and $P_1'-P_5'$, as shown in Fig. 7(a). The lines in the area around point M are too dense and tangled, so this area is redrawn in **Fig. 7(b)** for a closer view. When the coordinates of points P_1-P_5 and $P_1'-P_5'$ are determined, eqs. (30)-(47) allow the induction machine's performance extreme values to be obtained.

M 5.2. Numerical calculation

For the purpose of comparison, the algebraic method presented in paragraph 3, based on the T-type equivalent circuit of the motor shown in Fig. 2, is used to find the slip values and the corresponding extreme values. Except for the maximum torque and the maximum mechanical power, the slips at other performance extrema cannot be expressed analytically. Hence, numerical calculation is carried out. The procedure of the numerical calculation is straightforward. We write a characteristic, the torque in (3) for example, as a function of the slip s and the circuit parameters, and then set the derivative of this function to zero. Normally this leads to a high order nonlinear equation of s . The secant method is used to solve the equation and find the value of s . An initial guess of s is needed for the secant

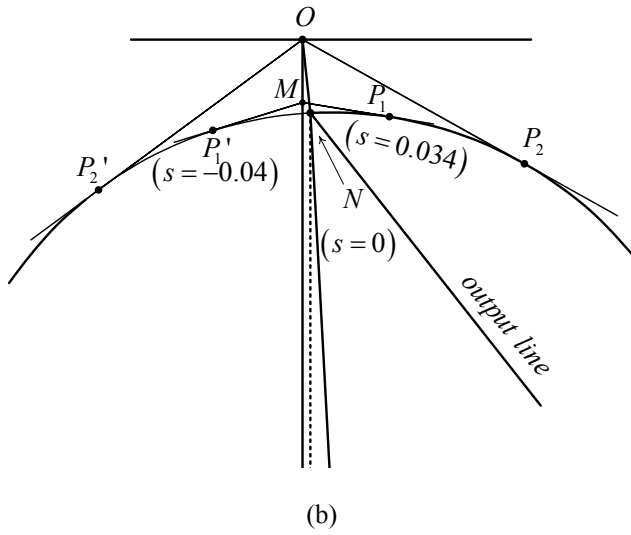


Fig. 7 : (a) Circle diagram of the illustrative example showing ten operation points of performance extrema. (b) A closer look at the circle diagram around points P_1 and P_1' , the maximum efficiency points.

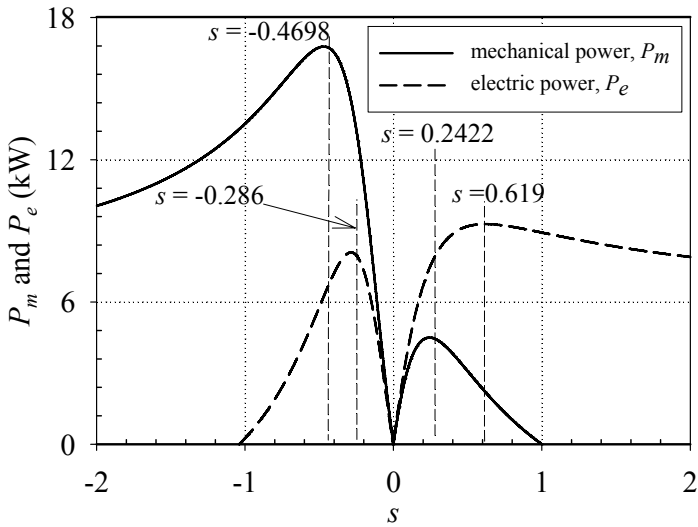


Fig. 8 : Mechanical and electric power vs. slip showing their extreme values and the corresponding slips

Table 1. Performance extreme values and corresponding slips calculated using numerical method

| Performance extremum | Motoring mode | Generating mode |
|--------------------------|---------------------|---------------------|
| maximum torque | $s_{TM}=0.3732$ | $s_{TG}=-0.3732$ |
| | $\tau_M=33.80$ N-m | $\tau_G=62.83$ N-m |
| maximum mechanical power | $s_{mp_M}=0.2422$ | $s_{mp_G}=-0.4698$ |
| | $P_{mM}=4499.5$ W | $P_{mG}=16769.5$ W |
| maximum power factor | $s_{PF_M}=0.125$ | $s_{PF_G}=-0.105$ |
| | $PF_M=0.872$ | $PF_G=0.81$ |
| maximum efficiency | $s_{\eta_M}=0.037$ | $s_{\eta_G}=-0.04$ |
| | $\eta_M=86.2$ % | $\eta_G=85.8$ % |
| maximum electric power | $s_{ep_M}=0.619$ | $s_{ep_G}=-0.286$ |
| | $P_{eM}=9284.2$ W | $P_{eG}=8088.76$ W |

Table 2. Comparison of performance extreme values obtained by algebraic and graphical methods

| Operating mode | Point | Method | Slip | Extremum | Error (%) |
|-----------------|--------|-----------|---------|----------------------|-----------|
| motoring mode | P_1 | algebraic | 0.037 | $\eta_M = 86.2$ % | 0.93 |
| | | graphical | 0.034 | $\eta_M = 85.4$ % | |
| | P_2 | algebraic | 0.125 | $PF_M=0.872$ | 0.23 |
| | | graphical | 0.126 | $PF_M=0.87$ | |
| | P_3 | algebraic | 0.24 | $P_{mM}=4499.5$ W | 0.36 |
| | | graphical | 0.23 | $P_{mM}=4515.5$ W | |
| | P_4 | algebraic | 0.3732 | $\tau_M = 33.80$ N-m | 0.68 |
| | | graphical | 0.37 | $\tau_M = 33.57$ N-m | |
| | P_5 | algebraic | 0.619 | $P_{eM}=9284.2$ W | 0.43 |
| | | graphical | 0.61 | $P_{eM}=9324.22$ W | |
| generating mode | P_1' | algebraic | -0.04 | $\eta_G = 85.8$ % | 1.4 |
| | | graphical | -0.04 | $\eta_G = 84.6$ % | |
| | P_2' | algebraic | -0.105 | $PF_G=0.81$ | 0.49 |
| | | graphical | -0.107 | $PF_G=0.806$ | |
| | P_3' | algebraic | -0.4698 | $P_{mG}=16769.5$ W | 0.67 |
| | | graphical | -0.46 | $P_{mG}=16657.6$ W | |
| | P_4' | algebraic | -0.3732 | $\tau_G = 62.83$ N-m | 0.02 |
| | | graphical | -0.37 | $\tau_G = 62.82$ N-m | |
| | P_5' | algebraic | -0.286 | $P_{eG}=8088.76$ W | 0.82 |
| | | graphical | -0.28 | $P_{eG}=8022.08$ W | |

6. Conclusion

This paper has presented two methods for calculating the performance extreme values of an induction machine working as a motor or a generator; the algebraic method and the circle diagram method, both methods give results which are in good agreement with each other. The algebraic method is a straightforward method that solves the induction machine equivalent circuit and finds the performance extrema using either the maximum power transfer theorem or the first derivative rule, the former applies to torque and mechanical power and allows the slip at an extremum and the corresponding extremum to be expressed in analytical forms, while the later applies to the rest of performance characteristics and requires resorting to numerical calculation for finding an extremum. The circle diagram method, although an old graphical method, is an easier and more intuitive method than the algebraic method for finding the performance extreme values. An illustrative example using the two methods to calculate the extrema of a practical induction machine has shown that the results obtained by the circle diagram method are as accurate as those obtained by the algebraic method.

The accurate results provided by the graphical method may surprise the reader since for a long time the circle diagram has been considered only capable of doing qualitative analysis of the induction machine. Thanks to the development of digital drawing tools, *i.e.*, Cad software, the graphical method is not only attractive as a tool for electrical engineers to quickly know the operational limits of an induction machine, but capable of giving accurate and reliable computation results. It is the authors' wish that with the use of modern graph drawing software the circle diagram method may find new applications in induction machine analysis.

References

- [1] S. J. Chapman, *Electric Machinery Fundamentals*: 3rd ed., McGraw-Hill, 1999.
- [2] A. E. Fitzgerald, C. Jr. Kingsley and S. D. Umans, *Electric Machinery*: 6th ed., McGraw-Hill, 2003.
- [3] G. McPherson and R. D. Laramore, *An Introduction to Electrical Machines and Transformers*: 2nd ed., Wiley, 1990.
- [4] J. Hindmarsh, *Electrical machines and their applications*: 4th ed., Pergamon Press, 1984.
- [5] D. L. Skaar, "Analysis of three-phase induction motors utilizing 'The Iodekice Locus' –a normalized impedance circle", *IEEE Trans. on Education*, Vol. 34, No. 4, pp. 336-342, 1991.
- [6] D. L. Skaar, "Analysis of single phase induction motors using the Iodekice Locus", *IEEE Trans. on Power Systems*, Vol. 9, No. 2, pp. 579-584, 1994.
- [7] D. L. Skaar, "Circumventing the blocked rotor test when evaluating model elements of three-phase induction motors", *IEEE Trans. on Energy Conversion*, Vol. 9, No. 2, pp. 397-403, 1994.
- [8] D. L. Skaar, "A simplified analysis of the six-element model of a three-phase induction motor", *IEEE Trans. on Education*, Vol. 41, No. 3, pp.232-234, 1998.
- [9] J. Chapallaz and J. D. Ghali, *Manual on induction motors used as generators*, Friedr Vieweg & Sohn Verlagsgesellschaft, Braunschweig, 2000.
- [10] S. Y. Huang and Y. J. Wang, "Analysis of a three-phase induction motor under voltage unbalance using the circle diagram method", *International Conference on Power System Technology*, Singapore, pp. 165-170, November 2004.
- [11] Y. J. Wang and S. Y. Huang "Determination of the performance extreme values of a three-phase induction motor using a graphical method", *International Journal of Electrical Engineering*, Vol. 16, No. 2, pp.101-109, 2009.
- [12] J. Lemke, *Microsoft Office Visio 2007 Step by Step*, Microsoft Press, 2007.